The dynamics of island nucleation and growth —beyond mean-field theory

P. A. Mulheran

Department of Physics, University of Reading
Whiteknights, Reading RG6 6AF, UK

PACS. 68.55.Jk – Structure and morphology; thickness; crystalline orientation and texture.
PACS. 81.15.Hi – Molecular, atomic, ion, and chemical beam epitaxy.
PACS. 05.40.-a – Fluctuation phenomena, random processes, noise, and Brownian motion.

Abstract. – Fully deterministic calculations of the dynamics of island nucleation and growth during thin-film deposition are presented, using a capture zone model that transcends the classical mean-field approximation. Nucleation rates for various critical island sizes $i = 0$, 1, 2 are accurately calculated from the time-dependent monomer density within the capture zones. The deterministic evolution of the Joint Probability Distribution (JPD) of island and capture zone size is then calculated. The JPDs are found to converge rapidly to approximately scale-invariant forms that are in excellent agreement with Monte Carlo simulation data.

Island nucleation and growth during thin-film deposition is often encountered, and is of widespread technological and scientific interest [1]. Islands can be used as the active elements in applications such as catalysis or electronics, and they are the building blocks of thin films and nanostructures. Scientific interest focuses on the statistical properties of the island arrays: How does the island density depend on coverage, deposition rate and temperature? What is the island size distribution and why does it display (to a very good approximation) scale invariance with coverage and deposition rate?

For decades the main theoretical approach to these questions has used mean-field rate equations [2–6], where islands of the same size are assumed to exist in the same environment, and success has been achieved in addressing the first of the questions concerning island density [5]. However, it has long been realised that this approach does not generally provide good predictions of the island size distribution, and cannot explain its scaling properties [6]. More recently, it has been shown that the island sizes are intimately related to their capture zones, which are the regions of substrate closest to the islands [7–9]. Material deposited into an island's capture zone is more likely to diffuse to that island that to any other, thereby dictating the island's growth rate. Therefore, a theory for the island size distribution must necessarily also consider the distribution of capture zones and how this varies as new islands nucleate, and so must look beyond the traditional mean-field approach.

A suitable theoretical approach has recently been suggested where the evolution of the Joint Probability Distribution (JPD) of island and capture zone sizes is considered [10, 11].

The JPD contains information on the spatial arrangement of the islands as well as their sizes, and so is a quantity of fundamental interest to both theory and experiment. The scale invariance of the JPD can be explained by assuming that the dynamics of the island density follow the mean-field results, and the detailed form of the JPD can then be successfully calculated for critical island size $i = 0$, 1, where islands of size greater than i are stable [10]. However, the reliance on the mean-field description of island nucleation rates is clearly not justified given the failings described above. (Other recent work using the capture zone picture to calculate the $i = 1$ island size distribution also relies on the mean-field dynamics [12]). In this paper we therefore examine the dynamics of island nucleation within the capture zone model, and show how nucleation rates can accurately be calculated for $i = 0$, 1, 2. In addition, these rates are used in entirely deterministic calculations [13] of the evolution of the JPDs. We find excellent agreement with simulation results for island density and the JPDs, and in particular we observe how the JPDs rapidly evolve to scale-invariant forms as previously predicted. Therefore this work provides a versatile and successful method of calculation that completely transcends the mean-field approach for the first time, and so significantly adds to our understanding of the statistical properties of island nucleation and growth.

We start by investigating the island nucleation rate within a single capture zone using Monte Carlo simulation (similar studies for island nucleation rates in one-dimension [14, 15] and on top of monolayer islands [16–18] have recently been carried out). The simulations are performed on a square lattice, with monomers being randomly deposited at a rate of F monolayers per unit time and diffusing with constant D. The behaviour of the simulation is dictated by the ratio $R = D/F$, and typically large values of $R \geq 10^5$ represent experimental conditions. In these simulations there is an absorbing circular island of radius $r_{\rm is}$ at the lattice origin, and the capture zone is a circle of radius $r_{\rm cz} > r_{\rm is}$. Thus, if a monomer diffuses within a distance $r_{\rm is}$ of the origin, it is completely removed from the simulation, whereas if it diffuses to a distance greater than $r_{\rm cz}$, it is removed but re-inserted at random at a distance $r_{\rm cz}$ from the origin. The latter process represents the fact that at a capture zone boundary the net flux of monomers is zero. Simulations start with no monomers in the capture zone, but the number of monomers rises as the simulation proceeds and will saturate if the simulation continues for a sufficient length of time. However, each simulation terminates if the conditions for the nucleation of a new island are satisfied. The condition for critical island size $i > 0$ is that $i+1$ monomers must coincide at a site at the same time. For spontaneous nucleation ($i = 0$) each monomer has a finite, low probability of causing a nucleation each time it takes a diffusive hop.

The simulation is repeated 1000 times for a range of $r_{\rm cz}$ and $r_{\rm is}$ so that the average time to nucleation can be estimated in each case to about 3% accuracy. From this we estimate the nucleation rate of each capture zone and island size pair in terms of a probability per diffusive hop. Typical results are shown in fig. 1a for $i = 0$, 1, 2. As expected, the nucleation rate decreases monotonically as the island radius increases, tending to zero as it approaches the capture zone radius.

In order to understand these nucleation rates, we calculate the monomer density profile $n_1(r, \theta)$ using the driven diffusion equation:

$$\frac{\partial n_1(r,\theta)}{\partial \theta} = 1 + R\nabla^2 n_1(r,\theta),$$

where $\theta = Ft$ is the fractional substrate coverage at time t after monomer deposition starts. This approach has been used before for $i = 1$ but assuming that the monomer density has saturated [19]; here we start with zero density. We implicitly use the circular symmetry of the island and capture zone system. From the monomer density we estimate the average time to nucleation $\langle\theta\rangle$, and hence nucleation rate $(4R\langle\theta\rangle)^{-1}$, by making a local-density approximation

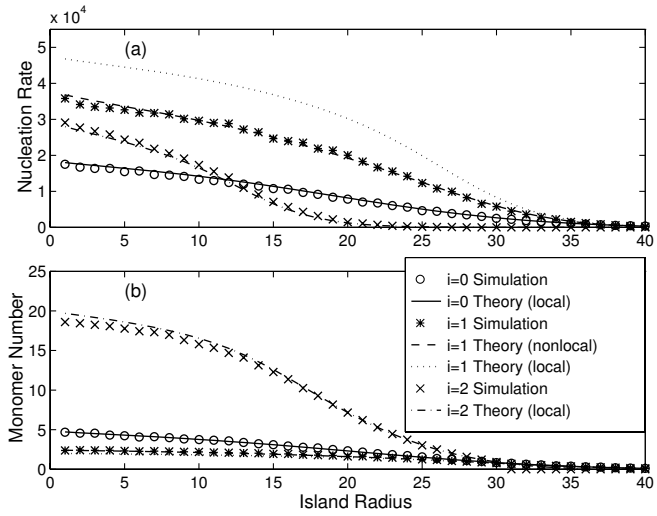

Fig. 1 – (a) Nucleation rates as a function of island radius. $i = 0$: $r_{\rm cz} = 50$, $R = 10^6$, probability of nucleation per diffusive hop is 3×10^{-5}; $i = 1$: $r_{\rm cz} = 50$, $R = 10^6$; $i = 2$: $r_{\rm cz} = 40$, $R = 10^5$. Parameters are selected to avoid the curves overlapping. "Theory (local)" lines are calculated using eq. (1). "Theory (nonlocal)" lines for $i = 1$ use averaged monomer density as described in the text. (b) The time-averaged monomer number in each of the cases in (a).

for nucleation probability $p_i(\theta)$ at each time-step:

$$p_i(\theta) = \int_{\rm is}^{\rm cz} \frac{n_1^{i+1}(r,\theta)}{i+1} 2\pi r \, {\rm d}r. \tag{1}$$

In this approximation we are assuming the arrivals of the $i + 1$ monomers at the same site are independent events. The utility of this approximation can be seen in fig. 1. The theory produces excellent results for $i = 0$ as expected, since here the nucleation is a single-particle event and obviously related to the monomer density profile as calculated above. Similarly, for $i = 2$ the theory produces excellent results; however, it fails for the case of $i = 1$. This failure has also been encountered before in one dimension [14, 15], in nucleation on top of monolayer islands [16–18], and in applications of the Level-Set method [20]. $i = 1$ is commonly encountered in experimental systems and therefore worthy of further investigation here.

To understand the reason for the relative success and failure of the theory for the different critical island sizes, in fig. 1b the time-averaged monomer number in each case is plotted. For $i = 2$, the monomer number is significantly greater than $i + 1$ for nearly all $r_{\rm is}$, and certainly is so for the low coverage of practical importance ($\theta \leq 0.3$), and therefore the local density approximation to the nucleation rate is a good one. As a consequence, we anticipate this theoretical approach will work equally well for higher critical island sizes $i > 2$ that are encountered in some systems [21]. However, for $i = 1$ the monomer number tends to saturate in the region of 2 monomers in the capture zone, since then a nucleation event is likely to occur. Here the local density approximation is very poor, since it allows the possibility of a single monomer interacting with itself to produce a nucleation event, which is why it overestimates the nucleation rate in fig. 1a.

To provide a better estimate for the $i = 1$ nucleation rate, we use the time and spatially averaged monomer density $\langle n_1 \rangle$ rather than the local one in the integral in eq. (1), since this

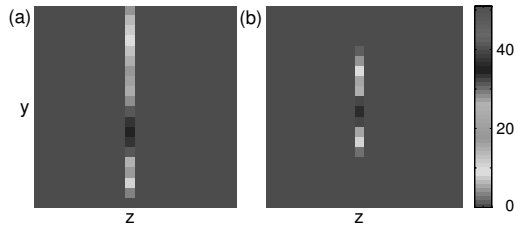

Fig. 2 – The initial forms of the JPD (multiplied by 4 and 2, respectively) used in the numerical solution of eq. (2), where the distribution of Voronoi areas is given by a Gamma Distribution [8] with parameter (a) $\beta = 3.61$ and (b) $\beta = 20$. In the plots the horizontal axis is the scaled island size z, the vertical axis the scaled capture zone area y, and the shading represents the value of the JPD in each bin.

compensates for the limited number of monomers in the system. In practice, the nucleation rate is first estimated and used to calculate $\langle n_1 \rangle$, which in turn is used to find a better estimate of the nucleation rate. The procedure is then repeated until a self-consistent solution is found. The results of this procedure are presented in fig. 1a, and it is clear that the agreement with the Monte Carlo rates is very satisfactory.

Having established reliable methods for calculating the nucleation rates in various capture zones, we can now proceed to calculate the evolution of the Joint Probability Distribution $f_i(a, s)$ of capture zone area a and island size s for various critical island sizes i during deposition [10, 11]. We shall assume that when a new island nucleates it fragments its parent capture zone taking a proportion λ of the area for its own zone and leaving the rest to the parent. This is the same fragmentation approximation used in earlier work; in reality, a new capture zone is formed from a number of nearest neighbours, but numerical work shows that this has little effect on the behaviour of the model [22]. In our earlier work we found that $\lambda = 0.4$ provides a good description of the fragmentation process and we use this value here. We also assume that the parent and daughter zones are created empty of monomers. From above, this is a reasonable approximation for $i = 1$ and also for other values of i at high island densities and substrate coverage. In other cases the monomer density soon saturates so its transients caused by the starting conditions are not significant. The evolution of $f_i(a, s)$ for $s > i + 1$ is then described by the following equation of motion:

$$\frac{\partial f_i(a,s)}{\partial \theta} = a[f_i(a, s-1) - f_i(a, s)] + 4R \cdot P_i\left(\frac{a}{1-\lambda}, s\right) \cdot f_i\left(\frac{a}{1-\lambda}, s\right) - 4R \cdot P_i(a, s) \cdot f_i(a, s), \quad (2)$$

where the first term represents deposition and subsequent capture by islands in capture zones of area a, and the following terms represent the creation and destruction, respectively, of capture zones through fragmentation. Islands of size $i + 1$ also have a source term from the nucleation events. The nucleation probability $P_i(a, s)$ can clearly be obtained from eq. (1) (and its variant for $i = 1$) by assigning $r_{\mathrm{cz}} = \gamma_i \sqrt{a/\pi}$, where γ_i is a geometric parameter that accounts for the fact that, in reality, capture zones are similar to Voronoi polygons [7–9] rather than circles; $r_{\mathrm{is}} = \sqrt{s/\pi}$ for the growth of circular islands.

Equation (2) can be solved numerically using an array of size 6000×500 to represent $f_i(a, s)$. The limit in size of the array means that the island density cannot be lower than about 5×10^{-4}, so the calculations all start with this density. The initial form of $f_i(a, s)$ depends on the earliest stages of island nucleation before spatial correlations are established, so a natural choice is for islands of size $s = i+1$ with a Random Voronoi Network distribution

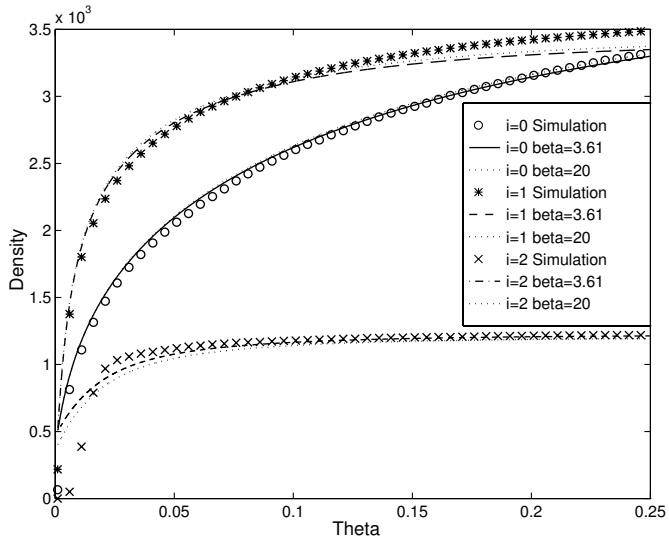

Fig. 3 – Island density as a function of substrate coverage θ. Theory lines, labelled by the value of β used in the initial conditions, are the solutions of eq. (2) with $\gamma_0 = 1.08$, $\gamma_1 = 1.03$ and $\gamma_2 = 1.15$.

of capture zone areas, as shown in fig. 2(a) using scaled island size $z = s/\overline{s}$ and scaled capture zone area $y = a/\overline{a}$. However, it is important to realise that the dynamics of the capture zone fragmentation dictate the long-time behaviour and are not very sensitive to the initial conditions. To demonstrate this point we also perform calculations starting with a much narrower distribution of capture zone areas shown in fig. 2(b).

Figure 3 shows the results from eq. (2) for the total island density as a function of the substrate coverage, using both starting conditions. For comparison we also plot data from Monte Carlo DDA (Deposition, Diffusion and Aggregation) simulations of the nucleation and growth of circular islands with various critical island sizes [8]. It is clear that very satisfactory agreement is found for all three values of i considered, and that the starting conditions have little impact on the overall behaviour.

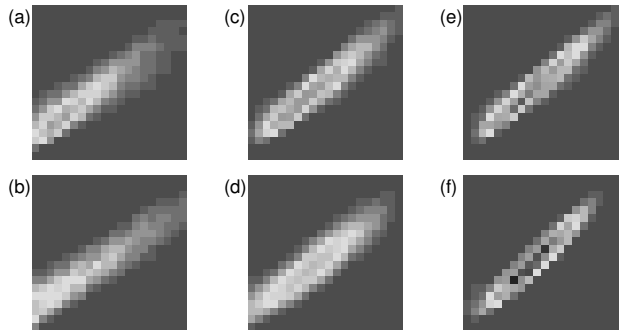

Fig. 4 – Scaled JPDs (multiplied by 10) drawn using the same axes and shading as in fig. 2. (a) and (b) for $i = 0$; (c) and (d) for $i = 1$; (e) and (f) for $i = 2$. The top row (a), (c) and (e) is calculated using eq. (2), and the bottom row (b), (d) and (f) are from DDA simulations, all at $\theta = 0.20$.

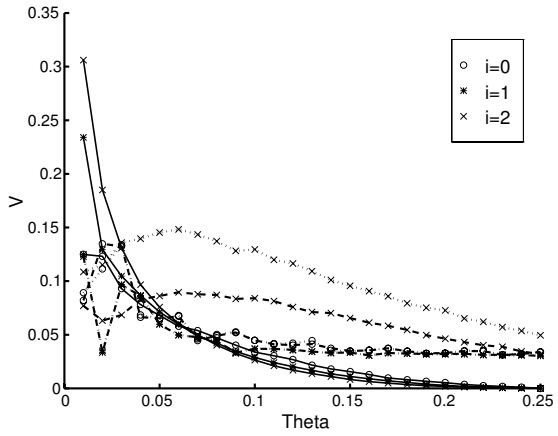

Fig. 5 – The solid line is $V = V_{\rm S}(\theta)$ (eq. (3)). Also shown is $V = V_{\rm T}(\theta)$ for $\beta = 3.61$ (broken line) and $\beta = 20$ (dotted line).

In fig. 4 we show the JPDs that evolve from the initial form (fig. 2a) for each value of i. It is clear that the nucleation and growth dynamics (eq. (2)) draw the JPDs into distinct forms that depend on critical island size i. The comparisons with the DDA simulation results are good for all cases; the JPDs lie along the $y = z$ diagonal, and become more peaked around $y = z = 1$ as the value of i increases. It should be noted that the JPDs provide a sensitive test of the theory, since they embody an order of magnitude more detail than the island size distribution alone modelled in other approaches [12].

In previous work [10], it was predicted that the JPDs should scale with coverage. We test this idea in fig. 5 by plotting the following integral:

$$V_{\rm S}(\theta) = \frac{\int\int [F_{\rm S}(y,z,\theta) - F_{\rm S}(y,z,0.25)]^2 \,{\rm d}y \cdot {\rm d}z}{\int\int [F_{\rm S}(y,z,\theta) + F_{\rm S}(y,z,0.25)]^2 \,{\rm d}y \cdot {\rm d}z}\,, \tag{3}$$

where $F_{\rm S}(y,z,\theta)$ is the simulated distribution of scaled capture zone area y and scaled island size z at coverage θ. It is clear that the DDA simulation does display approximate scaling $V_{\rm S} \approx 0$ for a wide range of θ ($V_{\rm S} = 1$ for two non-overlapping JPDs). To compare the calculated JPDs with the simulation data as the deposition proceeds we also show, in fig. 5,

$$V_{\rm T}(\theta) = \frac{\int\int [F_{\rm T}(y,z,\theta) - F_{\rm S}(y,z,\theta)]^2 \,{\rm d}y \cdot {\rm d}z}{\int\int [F_{\rm T}(y,z,\theta) + F_{\rm S}(y,z,\theta)]^2 \,{\rm d}y \cdot {\rm d}z}\,, \tag{4}$$

where $F_{\rm T}(y,z,\theta)$ is the theoretical JPD. It is clear that there is good agreement throughout. The initial conditions have a small effect on the $i = 2$ system, where the number of nucleation events is smallest (see fig. 3), but they are almost completely irrelevant to the $i = 0$, 1 systems where nucleation dynamics dominates.

Finally, we consider how the saturation island density depends on the ratio of diffusion to deposition rate R within this capture zone model. At the late stages of island growth the capture zones are long lived and the monomer density inside a zone of area a saturates at $n_1 \sim a/R$. Equation (1) implies that the nucleation rate $P_i \sim a^{i+2}/R^{i+1}$ for critical island size $i \neq 1$. Since the average capture zone area $a \sim 1/N$, the rate of change of island density $\dot{N} \sim RNP_i \sim N^{-(i+1)}R^{-i}$, so that the island density

$$N \sim R^{\frac{-i}{i+2}}. \tag{5}$$

This is in agreement with the accepted result from mean-field analyses [23] and DDA simulations. For $i = 1$, the argument is slightly modified following the use of $\langle n_1 \rangle$ in eq. (1), but we find $P_1 \sim N^{-3}R^{-2}$ and the result of eq. (5) still applies([1]).

From this work it is clear that entirely deterministic calculations for the statistical properties of island nucleation and growth during thin-film deposition can be made without recourse to the traditional mean-field approximation for the islands' environments. The dynamics, and the scaling of the saturation island density with deposition rate, are described well by the capture zone fragmentation model. In addition, the model provides detailed understanding of the forms and scaling with coverage of the Joint Probability Distributions of island and capture zone sizes. This is an area of almost complete failure for the traditional mean-field approach which we now suggest has been superseded by the capture zone model.

REFERENCES

[1] Kotrla M., Papanicolau N. I., Vvedensky D. and Wille L. T. (Editors), *Proceedings of the NATO ARW Atomistic Aspects of Epitaxial Growth, Corfu, 26-30 June 2001* (Kluwer, Dordrecht) 2002.
[2] Venables J. A., *Philos. Mag.*, **27** (1973) 693.
[3] Ratsch C., Zangwill A., Šmilauer P. and Vvedensky D. D., *Phys. Rev. Lett.*, **72** (1994) 3194.
[4] Amar J. G., Family F. and Lam P.-M., *Phys. Rev. B*, **50** (1994) 8781.
[5] Bales G. S. and Chrzan D. C., *Phys. Rev. B*, **50** (1994) 6057.
[6] Vvedensky D. D., *Phys. Rev. B*, **62** (2000) 15435.
[7] Mulheran P. A. and Blackman J. A., *Philos. Mag. Lett.*, **72** (1995) 55.
[8] Mulheran P. A. and Blackman J. A., *Phys. Rev. B*, **53** (1996) 10261.
[9] Bartelt M. C. and Evans J. W., *Phys. Rev. B*, **54** (1996) R17359; Bartelt M. C., Schmid A. K., Evans J. W. and Hwang R. Q., *Phys. Rev. Lett.*, **81** (1998) 1901.
[10] Mulheran P. A. and Robbie D. A., *Europhys. Lett.*, **49** (2000) 617.
[11] Evans J. W. and Bartelt M. C., *Phys. Rev. B*, **63** (2001) 235408.
[12] Amar J. G., Popescu M. N. and Family F., *Phys. Rev. Lett.*, **86** (2001) 3092.
[13] Zangwill A., *Nature*, **411** (2001) 651.
[14] Raffalle Vardavas, PhD Thesis, Imperial College of Science and Technology, 2002.
[15] Kallabis K., Krapivsky P. L. and Wolf D. E., *Eur. Phys. J. B*, **5** (1998) 801.
[16] Castellano C. and Politi P., *Phys. Rev. Lett.*, **87** (2001) 56102.
[17] Krug J., Politi P. and Michely T., *Phys. Rev. B*, **61** (2000) 14037.
[18] Heinrichs S., Rottler J. and Maass P., *Phys. Rev. B*, **62** (2000) 8338.
[19] Evans J. W. and Bartelt M. C., *Phys. Rev. B*, **66** (2002) 235410.
[20] Ratsch C., Gyure M. F., Chen S., Kang M. and Vvedensky D. D., *Phys. Rev. B*, **61** (2000) 10598.
[21] Swan A. K., Shi Z.-P., Wendelken J. F. and Zhang Z., *Surf. Sci.*, **391** (1997) L1205.
[22] Blackman J. A. and Mulheran P. A., *Comput. Phys. Commun.*, **137** (2001) 195.
[23] Blackman J. A. and Mulheran P. A., *From Quantum Mechanics to Technology*, edited by Petru Z., Przystawa J. and Papcewitz K., *Lect. Notes Phys.*, Vol. **477** (Springer-Verlag, Berlin) 1996, pp. 231-243.

([1])Here the nucleation rate varies with capture zone area as a^{i+2}, in agreement with [19] for $i = 1$, and contradicting an earlier approximation in [10].